

New tetraphenylethylene-containing conjugated polymers: Facile synthesis, aggregation-induced emission enhanced characteristics and application as explosive chemsensors and PLEDs

Wenbo Wu^a, Shanghui Ye^b, Runli Tang^a, Lijin Huang^a, Qianqian Li^a, Gui Yu^b, Yunqi Liu^{b,*}, Jingui Qin^a, Zhen Li^{a,*}

^a Department of Chemistry, Hubei Key Lab on Organic and Polymeric Opto-Electronic Materials, Luojia Street, Wuhan University, Wuhan 430072, China

^b Organic Solids Laboratories, Institute of Chemistry, The Chinese Academy of Sciences, Beijing 100190, China

ARTICLE INFO

Article history:

Received 26 February 2012

Received in revised form

6 May 2012

Accepted 18 May 2012

Available online 26 May 2012

Keywords:

Tetraphenylethylene (TPE)

Aggregation-induced emission

enhancement (AIEE)

Functional polyfluorene

ABSTRACT

In this paper, tetraphenylethylene (TPE) units, one of the typical aggregation-induced emission (AIE) moieties, are utilized to construct a new functional polyfluorene (PF) **P1**, which exhibited the exciting property of the aggregation-induced emission enhancement (AIEE), instead of the aggregation-caused quenching (ACQ) of normal PFs, and could probe the explosive with high sensitivity both in the nanoparticles and solid state. Three other TPE-containing polymers, **P2–P4**, were also successfully prepared, and demonstrated good performance as explosive chemosensors and light-emitting materials. **P3**, bearing carbazole as hole-transporting units showed the best performance with a maximum luminance efficiency of 1.17 cd/A and a maximum brightness of 3609 cd/m² at 12.9 V in its light-emitting diode device.

© 2012 Elsevier Ltd. All rights reserved.

1. Introduction

In the past decades, considerable interests have been attracted in the development of light-emitting diodes (LED) based on conjugated polymers, due to their wide-ranging applications [1]. Among them, polyfluorene (PF) and its derivatives are considered as promising light-emitting materials for their exceptionally high efficiencies both in photoluminescence (PL) and electroluminescence (EL) [2]. The high PL efficiencies also make some specific functional PFs widely used in other fields, for example, chemosensors [3]. However, PFs are likely to aggregate and form excimers in solid states, directly leading to the fluorescence quenching, namely aggregation-caused quenching (ACQ) [4], hence inhibiting their prospective utilizations in a large degree. Although many different approaches including chemical, physical, and engineering ones have been attempted to hamper these luminophore aggregations, they are still a little far from ideal, because the ACQ effect is alleviated at the expense of other useful properties [5]. Thus, it is badly needed to change the ACQ property of PFs, without sacrificing

other advantages. For chemists, the general approach is to modify the structure at the molecular level.

Tetraphenylethylene (TPE) is characterized by its aggregation-induced emission (AIE) attribute [6], which was first reported by Tang's group [7a]: it is virtually nonluminescent when molecularly dissolved in its good solvents, but emits intensely when aggregated in its poor solvents or fabricated into thin solid film [7]. This is exactly opposite to the ACQ effect, and has recently been given much attention due to the huge potential high-tech applications in many areas [8]. Thus, if the TPE unit was introduced into the PF system, perhaps, the original ACQ behavior might be converted to AIE(E) phenomena. However, the related reports were very scarce. Inspired by this idea, in this paper, a new functional PF **P1** (Chart 1), containing the TPE moieties in the main chain, was therefore synthesized through typical Pd-catalytic Suzuki polymerization. As expected, the light-emitting behavior of **P1** was not ACQ any longer, but aggregation-induced emission enhancement (AIEE). That was to say, in solution, **P1** could emit weak fluorescence, however, the emission was enhanced largely in solid state including nanoparticles and thin films. And it could be used as chemsensors for the detection of explosives. Furthermore, other three TPE-containing polymers, **P2–P4** (Chart 2), were successfully prepared, in which the spirobifluorene, carbazole and 1,3,4-oxadiazole moieties were

* Corresponding authors. Fax: +86 27 68756757.

E-mail addresses: liuyq@iccas.ac.cn (Y. Liu), lizhen@whu.edu.cn (Z. Li).

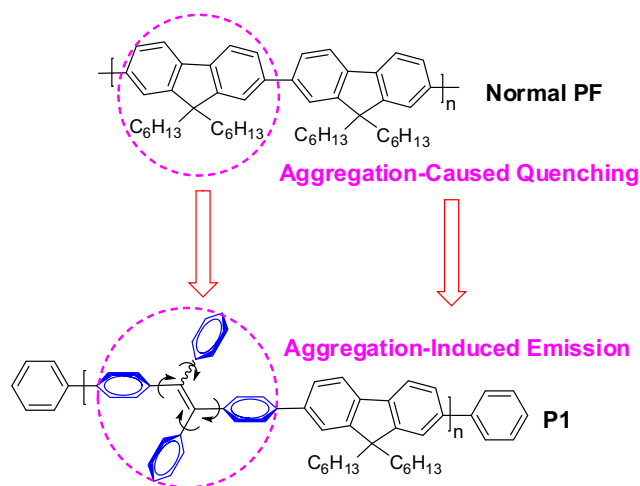


Chart 1. The sketch map from normal PF to TPE-containing P1.

used as comonomers, to further investigate the above idea and improve the LED performance. All these polymers possessed AIEE characteristic, and act as good chemosensors and light-emitting materials. Herein, we would like to present their synthesis, characterization, AIEE properties, sensing behavior, and LED device performance in detail.

2. Experimental section

2.1. Materials

Tetrahydrofuran (THF) was dried over and distilled from K-Na alloy under an atmosphere of dry nitrogen. Pyridine was dried over from CaH_2 and distilled under normal pressure before use. 9,9-Dihexylfluorene-2,7-bis(trimethyleneborate) (**S4**) was purchased from Aldrich while the other two boronic esters **S5** and **S6** were prepared through the same synthetic routes reported in the literature [9]. 2,5-Di(4-bromobenzoyl)-1,3,4-oxadiazole (**S5**) was also synthesized according to our previous work [1f]. 2-Isopropoxy-4,4,5,5-tetramethyl-1,3,2-dioxaborolane was purchased from Aldrich, while *n*-butyllithium (2.6 M in hexane) and 4-bromo-

benzophenone (**S1**) were bought from Alfa-Aesar. All other reagents were used as received.

2.2. Instrumentation

^1H and ^{13}C NMR spectra were measured on a Varian Mercury300 spectrometer or Varian Mercury600 spectrometer using tetramethylsilane (TMS; $\delta = 0$ ppm) as internal standard. The Fourier transform infrared (FT-IR) spectra were recorded on a Perkin Elmer-2 spectrometer in the region of $4000\text{--}400\text{ cm}^{-1}$ on KBr pellets. UV-visible spectra were obtained using a Shimadzu UV-2550 spectrometer. FAB-MS spectra were recorded with a VJ-ZAB-3F-Mass spectrometer. Elemental analyses were performed by a CARLOERBA-1106 micro-elemental analyzer. Photoluminescence spectra were performed on a Hitachi F-4500 fluorescence spectrophotometer. Gel permeation chromatography (GPC) was used to determine the molecular weights of polymers. GPC analysis was performed on a Waters HPLC system equipped with a 2690D separation module and a 2410 refractive index detector. Polystyrene standards were used as calibration standards for GPC. THF was used as an eluent and the flow rate was 1.0 mL/min. Thermal analysis was performed on NETZSCH STA449C thermal analyzer at a heating rate of $10\text{ }^\circ\text{C}/\text{min}$ in nitrogen at a flow rate of $50\text{ cm}^3/\text{min}$ for thermogravimetric analysis (TGA). The thickness of the films was measured with an Ambios Technology XP-2 profilometer. Electrochemical Workstation with a Pt disk, a Pt plate, and a Ag/Ag^+ electrode as the working electrode, counter electrode and reference electrode, respectively, in a 0.1 mmol/mL tetrabutylammonium hexafluorophosphate (Bu_4NPF_6) acetonitrile solution. Scanning electron microscopy (SEM) was performed on a QUANTA scanning electron microscope (FEI Co., Netherlands), and the nanoaggregate thin films were prepared by its THF/water (1/9 v/v) suspension (0.02 mg/mL in THF) dropped on the slides and dried at about $60\text{ }^\circ\text{C}$.

2.3. Synthesis of 1,2-bis(4-bromophenyl)-1,2-diphenylethene (**S2**)

To a mixture of Zn (3.90 g, 60.0 mmol) and 40 mL of dry THF was added TiCl_4 (3.3 mL, 30.0 mmol) under an atmosphere of argon at $0\text{ }^\circ\text{C}$. The mixture was stirred for 30 min at room temperature and another 2 h at $60\text{ }^\circ\text{C}$, then 4-bromobenzophenone (**S1**) (0.85 mg, 2.5 mmol) in 30 mL of THF with pyridine (1 mL) was added dropwise in 1 h at $0\text{ }^\circ\text{C}$. The mixture was refluxed overnight. After

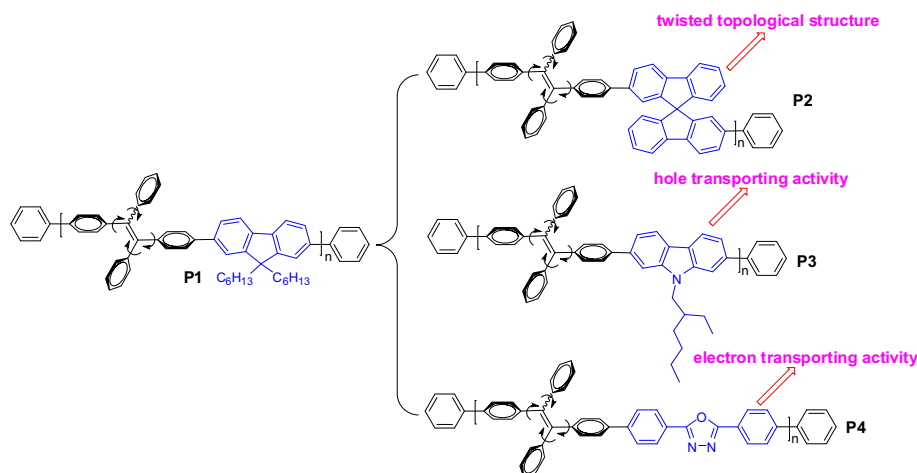


Chart 2. The different chemical structures from P1 to polymers P2–P4.

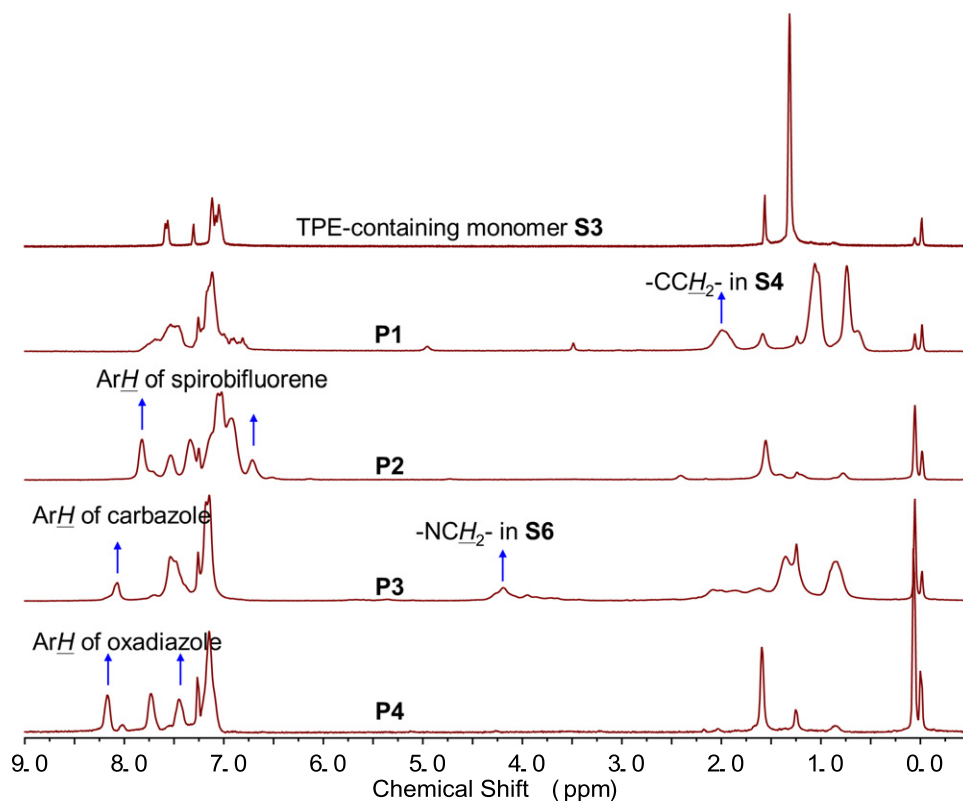


Fig. 1. The ^1H NMR spectra of polymers **P1**–**P4** and monomer **S3** conducted in chloroform-*d*.

cooling to room temperature, 10% K_2CO_3 (aq) was added and the mixture was filtrated. The filtrates were extracted with CH_2Cl_2 and the extracts were collected, combined, and washed with brine and dried over anhydrous Na_2SO_4 . After removal of the solvents under reduced pressure, the crude product was purified by column chromatography on silica gel using chloroform/petroleum ether (1/5, V/V) as eluent to afford white solid (1.12 g, 76.2%). IR (KBr), ν (cm^{-1}): 1584 (C=C). ^1H NMR (300 MHz, CDCl_3 , 298 K), δ (TMS, ppm): 6.87 (d, $J = 5.1$ Hz, 4H, ArH), 6.99 (s, br, 4H, ArH), 7.10 (s, br, 6H, ArH), 7.20 (d, $J = 5.1$ Hz, 4H, ArH). ^{13}C NMR (75 MHz, CDCl_3 ,

298 K), δ (TMS, ppm): 120.6, 126.9, 127.7, 128.0, 130.8, 131.2, 132.8, 140.2, 142.3, 142.7. MS (FAB), m/z [M^+]: 487.97, calcd: 487.98. $\text{C}_{26}\text{H}_{18}\text{Br}_2$ (EA) (%), found/calcd): C, 62.71/63.70; H, 3.95/3.70.

2.4. Synthesis of 1,2-diphenyl-1,2-bis(4-(4,4,5,5-tetramethyl-1,3,2-dioxaborolan-2-yl)phenyl)ethane (**S3**)

To a solution of **S2** (980 mg, 2.0 mmol) in 40 mL dry THF at -78°C , 2.2 mL of *n*-butyllithium (2.6 M in hexane, 5.7 mmol) was

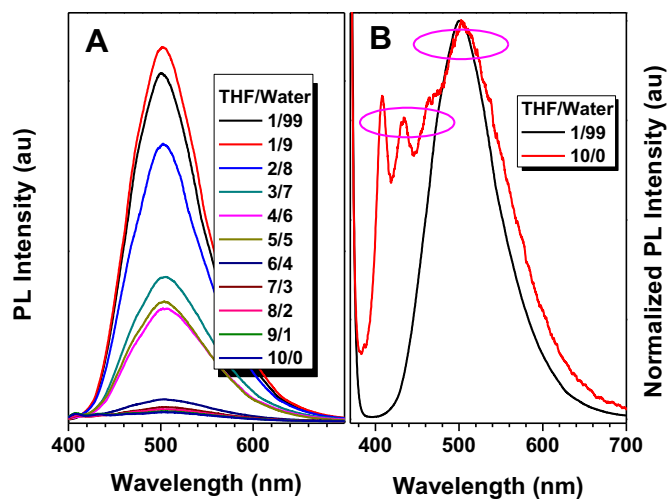


Fig. 2. A: Photoluminescence (PL) spectra of **P1** in THF and THF/water mixtures (2.0×10^{-3} mg/mL, $\lambda_{\text{ex}} = 377$ nm); B: Normalized PL spectra of **P1** in the solution and aggregate states.

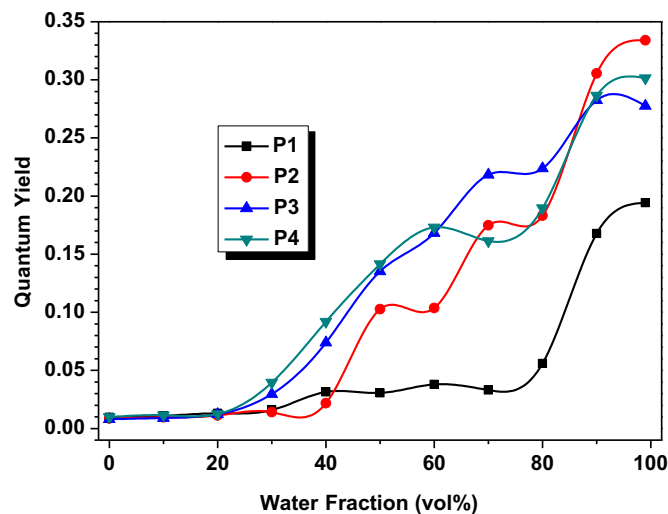


Fig. 3. Variations in the fluorescence quantum yields (Φ_F) of **P1**–**P4** with water fractions in the THF/water mixtures. 9,10-diphenylanthracene in cyclohexane ($\Phi_F = 90\%$) as reference.

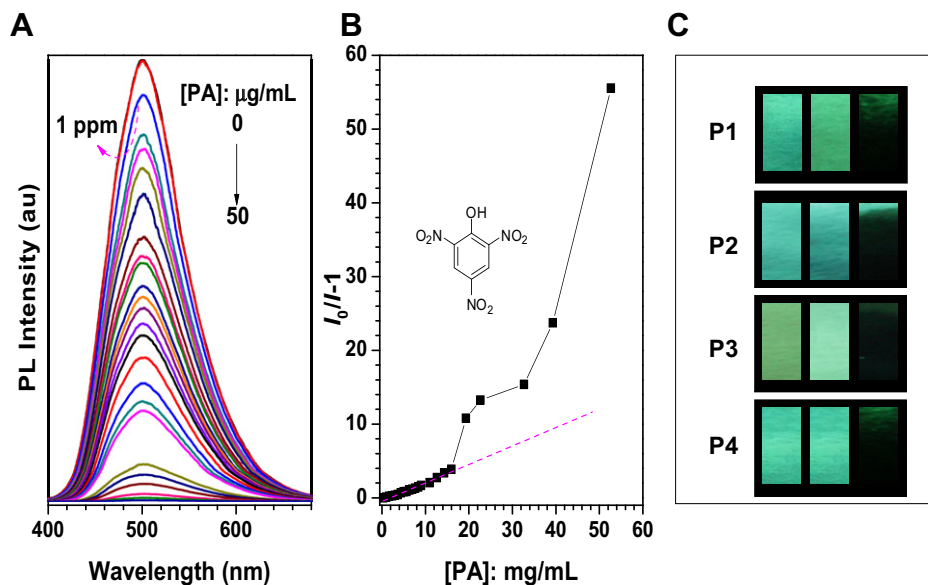


Fig. 4. A: PL spectra of **P1** in THF/water mixture (1:9 v/v 2.0×10^{-3} mg/mL) containing different amounts of picric acid (PA); B: PA concentration effect on the PL peak intensity of **P1** in THF/water mixture (1:9 v/v 2.0×10^{-3} mg/mL), where I = peak intensity and I_0 = peak intensity at [PA] = 0 mg/mL; Inset of B: The structure of PA; C: fluorescence images of **P1–P4** adsorbed in the filter papers before (the left one), after (the middle one) being partially dipped into pure toluene and after (the right one) being partially dipped into a toluene solution of PA (**P1** and **P2**: 60 $\mu\text{g/mL}$; **P3** and **P4**: 50 $\mu\text{g/mL}$).

added dropwise. The mixture was stirred at -78°C for 2 h. Then, 2.2 mL of 2-isopropoxy-4,4,5,5-tetramethyl-1,3,2-dioxaborolane (9.6 mmol) was added rapidly to the above solution and the mixture was stirred for 2 h. The resulting mixture was warmed up to room temperature and stirred for 24 h, then poured into water, and extracted with chloroform. The combined extracts were washed with brine, dried over anhydrous Na_2SO_4 , and concentrated. The crude product was purified by column chromatography on silica gel using ethyl acetate/petroleum ether (1:10) as eluent to afford white powder **S3** (438 mg, 37.8%). IR (KBr), ν (cm^{-1}): 1606 (C=C). ^1H NMR (300 MHz, CDCl_3 , 298 K), δ (TMS, ppm): 1.32 (s, 24H, $-\text{CH}_3$), 7.0–7.1 (m, 14H, ArH), 7.53 (d, $J = 7.2$ Hz, 4H, ArH). ^{13}C NMR (75 MHz, CDCl_3 , 298 K), δ (TMS, ppm): 25.1, 83.4, 126.7, 127.8, 127.9, 130.9, 131.5, 134.2, 124.3, 141.4, 143.5, 146.9. MS (FAB), m/z [M^+]: 584.35, calcd: 584.33. $\text{C}_{38}\text{H}_{42}\text{B}_2\text{O}_4$ (EA) (% found/calcd): C, 78.83/78.10; H, 7.24/7.24.

2.4.1. Synthesis of **P1**

A mixture of 9,9-dihexylfluorene-2,7-bis(trimethyleneborate) (**S4**) (125.6 mg, 0.25 mmol), monomer **S2** (122.6 mg, 0.25 mmol), sodium carbonate (265 mg, 2.5 mmol), THF (7.5 mL)/water (1.25 mL), and $\text{Pd}(\text{PPh}_3)_4$ (4.0 mg) was carefully degassed and charged with argon. Then the reaction mixture was stirred at 60°C for 3 days. Then, the trace end groups were capped by refluxing for 12 h with phenylboronic acid and bromobenzene sequentially. A lot of methanol was poured into the mixture, then filtered. The obtained solid was dissolved in THF, and the insoluble solid was filtered out. After removal of the solvent, the residue was further purified by several precipitations from THF into acetone, and the obtained solid was then washed with a lot of acetone and dried in a vacuum at 40°C to a constant weight. The resultant polymer was obtained as dark green powder (113.2 mg, 68.4%). $M_w = 10,900$, $M_w/M_n = 1.76$ (GPC, polystyrene calibration). IR (KBr), ν (cm^{-1}): 1604 (C=C). ^1H NMR (300 MHz, CDCl_3 , 298 K), δ (TMS, ppm): 0.6–1.0 ($-\text{CH}_3$), 1.0–1.4 ($-\text{CH}_2-$), 1.8–2.2 ($-\text{CCH}_2-$), 6.8–7.3 (ArH), 7.3–7.8 (ArH). ^{13}C NMR (75 MHz, CDCl_3 , 298 K), δ (TMS, ppm): 14.3, 22.8, 24.0, 30.0, 31.7,

40.7, 55.5, 110.4, 114.3, 120.2, 121.3, 126.5, 128.2, 131.1, 131.6, 132.0, 133.3, 139.6, 140.3, 132.0, 151.9.

2.4.2. Synthesis of **P2**

The synthesis of **P2** was similar as **P1**. **S2** (62.1 mg, 0.127 mmol), bromic ester **S5** (72.0 mg, 0.127 mmol), sodium carbonate (134.3 mg, 1.27 mmol), THF (3.9 mL)/water (0.65 mL), and $\text{Pd}(\text{PPh}_3)_4$ (2.0 mg). The resultant polymer was obtained as pale green powder (57.1 mg, 69.9%). $M_w = 5700$, $M_w/M_n = 1.53$ (GPC, polystyrene calibration). IR (KBr), ν (cm^{-1}): 1601 (C=C). ^1H NMR (300 MHz, CDCl_3 , 298 K), δ (TMS, ppm): 6.5–6.7 (ArH), 6.7–7.4 (ArH), 7.4–7.6 (ArH), 7.6–7.8 (ArH). ^{13}C NMR (150 MHz, CDCl_3 , 298 K), δ (TMS, ppm): 120.2, 120.4, 122.5, 124.2, 126.2, 126.3, 126.4, 126.5, 126.6, 126.9, 127.0, 127.3, 127.8, 127.9, 128.8, 130.9, 131.5, 131.6, 131.8, 131.9, 138.6, 140.5, 140.6, 140.8, 141.1, 141.6, 142.0, 142.8, 142.9, 143.8, 148.8, 149.3, 149.5.

2.4.3. Synthesis of **P3**

The synthesis of **P3** was similar as **P1**. **S2** (122.6 mg, 0.25 mmol), bromic ester **S6** (132.8 mg, 0.25 mmol), sodium carbonate (265 mg, 2.5 mmol), THF (7.5 mL)/water (1.25 mL), and $\text{Pd}(\text{PPh}_3)_4$ (4.0 mg). The resultant polymer was obtained as yellow powder (122.0 mg, 80.3%). $M_w = 11,000$, $M_w/M_n = 1.91$ (GPC, polystyrene calibration). IR (KBr), ν (cm^{-1}): 1601 (C=C). ^1H NMR (300 MHz, CDCl_3 , 298 K), δ (TMS, ppm): 0.6–1.0 ($-\text{CH}_3$), 1.0–1.4 ($-\text{CH}_2-$), 1.5–2.1 ($-\text{CH}_2-$), 3.8–4.3 ($-\text{NCH}_2-$), 6.9–7.2 (ArH), 7.2–7.6 (ArH), 7.9–8.2 (ArH). ^{13}C NMR (150 MHz, CDCl_3 , 298 K), δ (TMS, ppm): 11.3, 14.3, 23.3, 24.7, 29.0, 31.2, 39.6, 47.5, 107.4, 118.7, 120.7, 122.1, 126.8, 127.1, 128.0, 128.1, 129.0, 131.8, 132.2, 138.6, 140.1, 141.0, 142.3, 142.9, 144.2.

2.4.4. Synthesis of **P4**

The synthesis of **P4** was similar as **P1**. **S3** (116.9 mg, 0.20 mmol), **S7** (76.0 mg, 0.20 mmol), potassium carbonate (276 mg, 2.0 mmol), THF (6 mL)/water (1 mL), and $\text{Pd}(\text{PPh}_3)_4$ (3.2 mg). The resultant polymer was obtained as yellow powder (65.1 mg, 59.1%). $M_w = 5600$, $M_w/M_n = 1.66$ (GPC, polystyrene calibration). IR (KBr), ν (cm^{-1}): 1609 (C=C). ^1H NMR (300 MHz, CDCl_3 , 298 K), δ (TMS, ppm): 7.0–7.3 (ArH), 7.4–7.5 (ArH), 7.6–7.8 (ArH), 8.1–8.3 (ArH). ^{13}C

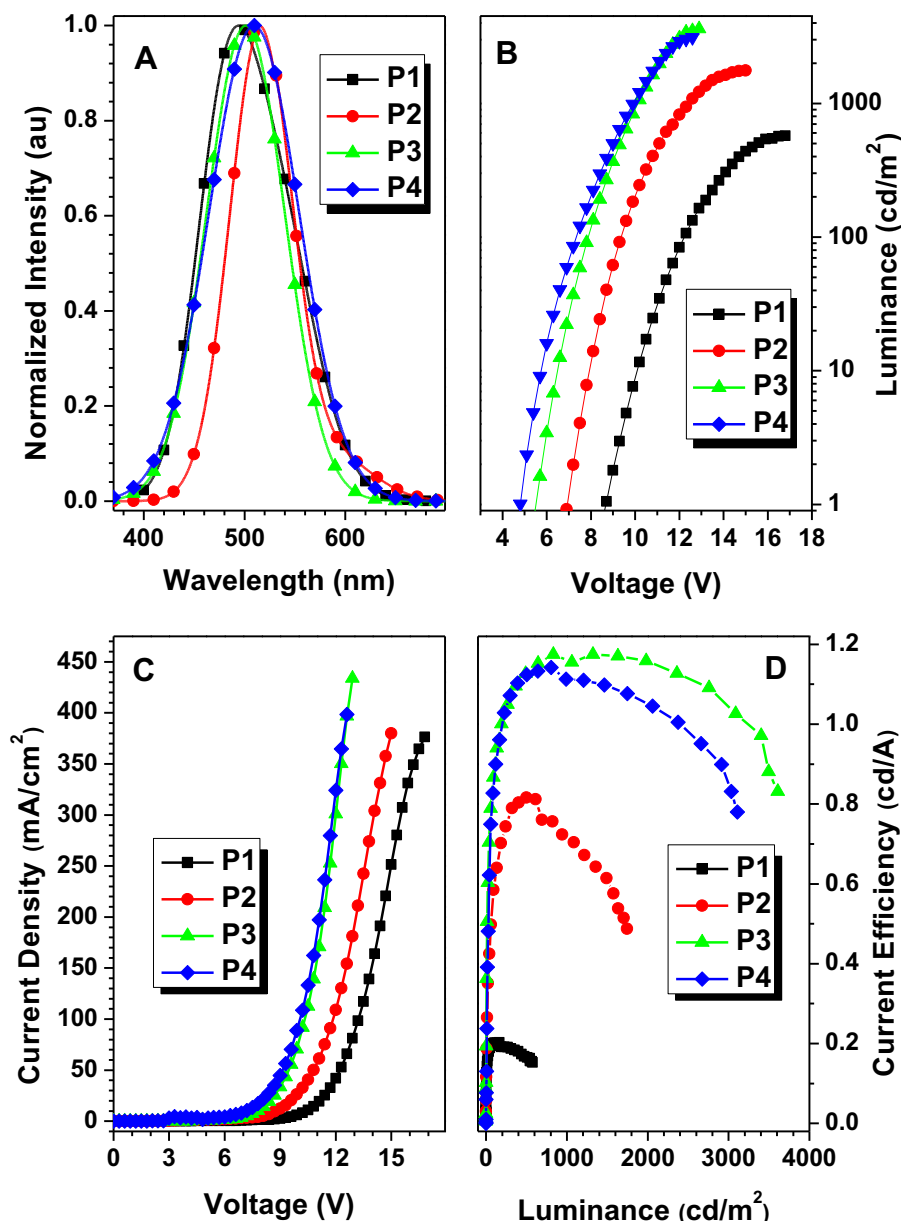


Fig. 5. A: The EL spectra of P1–P4; B: Luminance–voltage characteristics of the PLED devices; C: Current–voltage characteristics of the PLED devices; D: The luminescence efficiency–current characteristics of PLED devices.

NMR (150 MHz, CDCl₃, 298 K), δ (TMS, ppm): 122.7, 126.8, 127.7, 127.9, 128.1, 131.7, 132.4.

2.4.5. Fabrication and characterization of PLEDs

In a general procedure, indium-tin oxide (ITO)-coated glass substrates were etched, patterned, and washed with detergent, deionized water, acetone, and ethanol sequentially. We fabricated PLEDs using these polymers P1–P4 as the emissive layer with a structure of ITO/PEDOT:PSS (25 nm)/Poly-TPD (25 nm)/EML (32 nm)/TPBI (35 nm)/Cs₂CO₃ (8 nm):Ag (100 nm), (ITO was indium-tin oxide; PEDOT was poly(3,4-ethylenedioxythiophene); PSS was poly(styrenesulfonate); TPD was *N,N'*-Bis(3-methylphenyl)-*N,N'*-bis(phenyl)-benzidine and TPBI was 1,3,5-tris(N-phenylbenzimidazol-2-yl)benzene), where PEDOT:PSS, Poly-TPD and TPBI were used as hole injection, electron-blocking/hole-transporting and hole-blocking/electron-transporting layer,

respectively. The active layer was spin-coated from chlorobenzene solution and TPBI layer was deposited by means of conventional vacuum deposition onto the ITO coated glass substrates at a pressure of 8×10^{-5} Pa. The active area of device was 5 mm². A quartz crystal oscillator placed near the substrate was used to monitor the thickness of each layer, which was calibrated ex situ using an Ambios Technology XP-2 surface profilometer. UV–vis absorption and fluorescence spectra were collected with a Hitachi U-3010 and Hitachi F-4500 spectrophotometer, respectively. EL spectra and chromaticity coordinates were measured with a SpectraScan PR650 photometer. Current density–voltage–luminance (*J*–*V*–*L*) measurements were made simultaneously using a Keithley 4200 semiconductor parameter analyzer and a Newport multifunction 2835-C optical meter, with luminance measured in the forward direction. All device characterizations were carried out under ambient laboratory air at room temperature.

3. Results and discussion

3.1. Synthesis and characterizations

As shown in Scheme 1, the bromized TPE **S2** was prepared via McMurry Olefination from 4-bromobenzophenone (**S1**). The reaction underwent smoothly, and the desired compound was obtained in the yield of 76.2%. Then, during normal procedure for the preparation of boronic ester [9], **S3** was obtained as white solid. Other comonomers were obtained by following the reported procedures [1f,9], and the synthetic routes were listed in Scheme S1 in supporting information. The synthetic route of polymers **P1–P4** was shown in Scheme 2, and the polymerization procedure was proceeded smoothly through the typical Suzuki coupling reaction using Pd(PPh₃)₄ as a catalyst, sodium carbonate (aq) as a base, and THF as the solvent. After three days, the end-capped groups (phenylboronic acid and bromobenzene) were added to react with the bromo- and boronic ester end groups (which might quench the fluorescence of the resultant polymers) [1]. **P1–P4** were obtained with satisfied yields (Table 1), and they were readily soluble in common organic solvents, such as THF, CHCl₃, etc.

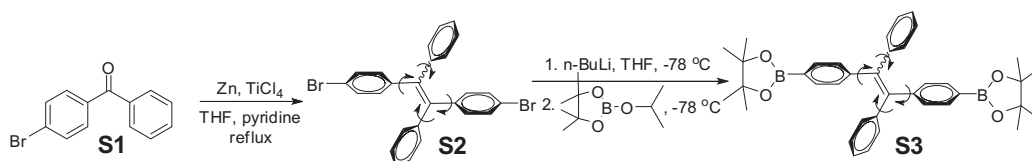
The molecular structures of these four polymers **P1–P4** were characterized by “wet” spectroscopic techniques, and the detailed spectral analysis data for them were given in the experimental section and supporting information. Fig. S1 (in the supporting information) showed their FT-IR spectra. The TPE-containing compound **S2** exhibited an absorption band at around 1605 cm⁻¹, which could be assigned to the stretching vibrations of C=C. The appearance of the stretching vibration of C=C in the IR spectra of the polymers indicated that the TPE moieties were successfully introduced.

Fig. 1 showed the ¹H NMR spectra of polymers **P1–P4**, which were conducted in the solvent of chloroform-*d*. All the peaks could be readily assigned to the resonances of appropriate protons of these polymers (Scheme 2), and no unexpected peaks appeared. Except the resonance peaks of TPE unit, there were still some characteristic peaks assigned to the resonances of protons of the other comonomers, which were marked in Fig. 1, indicating the Suzuki polymerization were successful. Taking **P3**, containing carbazole as comonomer, as an example: the ArH signals of TPE unit were at about $\delta = 7.0$ and 7.5 ppm; except that, there were also some new peaks assigned to the protons of ArH in carbazole (typically at about $\delta = 8.3$ ppm) and the NH₂ protons at about $\delta = 4.3$ ppm, as well as some CH₂ peaks in the range of $\delta = 0.8$ –2.0, indicating this polymer was derived from TPE moieties and carbazole moieties. And due to the polymerization, all the peaks showed an inclination of signal broadening. In their ¹³C NMR spectra (see supporting information and experimental section), the similar phenomenon was also observed. In **P3**, except the signals of TPE unit, some alkyl carbon signals and aromatic carbon signals, which should be derived from carbazole moieties, appeared. In addition, the peaks at about 25 and 83 ppm, typical signals of the boronic ester group, disappeared completely, also indicating the successful polymerization.

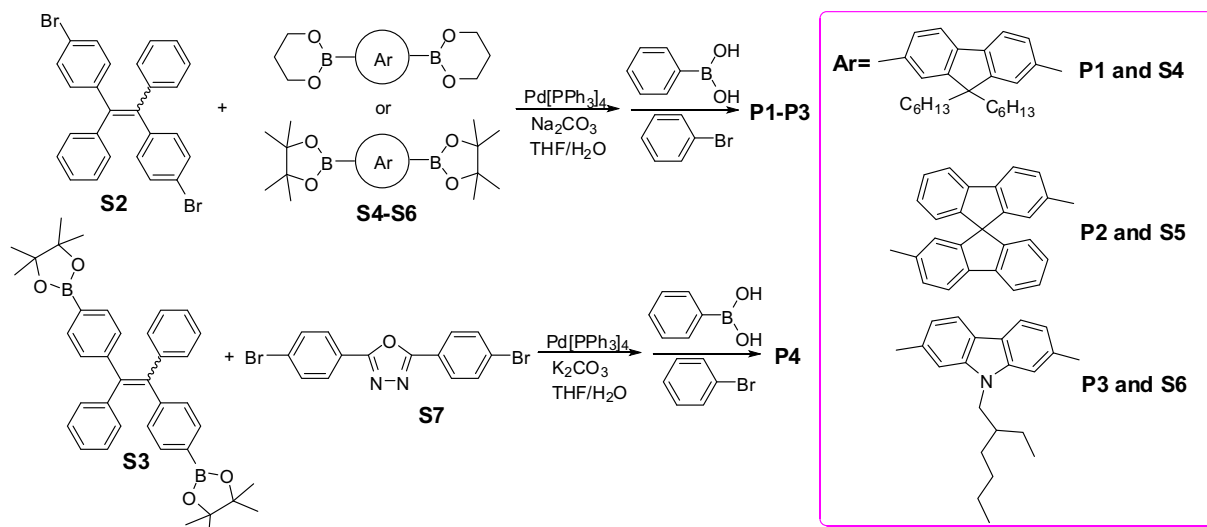
The molecular weights of **P1–P4**, determined by gel permeation chromatography (GPC) with THF as an eluent and polystyrene standards as calibration standards, were listed in Table 1 and experimental section. Here, **P2** and **P4**, only constructed by rigid aromatic rings, demonstrated lower molecular weights than those of **P1** and **P3**, possibly due to their relative poor solubility. Actually, during the polymerization procedure of **P4**, some insoluble polymer was also yielded, indicating that the soluble fractions with high molecular weights could not be obtained. Their thermal gravimetric analysis (TGA) thermograms were shown in Fig. S10, with the 5% weight loss temperature (*T_d*) summarized in Table 1. All the polymers were thermolytically resistant, and the *T_d* values were all higher than 360 °C. Here, the rigid structure demonstrated the advantage of good stability, for example, the *T_d* value of **P2** was as high as 473 °C. Also, the glass transition temperature (*T_g*) were investigated by using a differential scanning calorimeter (DSC) technology. It was a pity that the glass transition temperatures of nearly all the polymers were not obvious in the DSC curve except **P1** (143 °C). Since the structure of **P2** and **P4** were much more rigid than **P1**, we could conjecture that their *T_g* values may be even higher than 143 °C, while **P3** might have a similar *T_g* value as **P1**.

3.2. Optical properties and AIEE effects

As mentioned above, the original goal of the introduction of TPE moieties to PF, was to change its properties from ACQ to AIE effect. Thus, we attempted to investigate the photoluminescence (PL) behaviors of **P1–P4** in the solution and aggregate states. The aggregates were prepared by adding distilled water into their THF solutions under vigorous stirring. The resultant mixtures were visually transparent and macroscopically homogenous, suggesting that the polymer aggregates were nanometer-sized [10]. When illuminated with a UV lamp ($\lambda = 365$ nm), there was nearly none fluorescence emitted from the dilute THF solution of **P1**, while a very weak sky blue fluorescence observed from its concentrated solutions. But the emission became much stronger in its aggregate states and solid films, and the fluorescence became green light. To verify the visual observations, the UV–vis and PL spectra were studied. As shown in Fig. S11 (Supporting Information), the UV–vis spectra of **P1** in pure THF and THF/water mixtures exhibited similar profiles. However, the PL behaviors were quite different. Upon excitation at 377 nm, **P1** was a very weak emitter when molecularly dissolved in pure THF (Fig. 2A). In contrast, when a large amount of water was added into the solution, an intense PL peak centered at 503 nm was recorded under the same measurement conditions (Fig. 2A). Meanwhile, its normalized PL spectra in the solution and aggregate state were showed in Fig. 2B. It was easily seen that in its PL spectra in aggregate state, there was only one main peak centered at 503 nm, while in the solution, except this peak, there were still some small ones. It was understandable. First, we could confirm that the peak around 503 nm was the emission of the aggregated particles, since only this peak remained in the aggregate state and dramatically enhanced in comparison with that in the solution, similar to the optical properties of TPE. As well known, the



Scheme 1. Synthesis of monomers **S2** and **S3**.

Scheme 2. Synthesis of TPE-containing polymers **P1–P4**.

AIE effect was considered to be induced by the restriction of the intramolecular rotation (IMR) process of the luminophore [7a,7b,11]. In the case of TPE, its four phenyl rings underwent an active IMR process in the solution state, thus, quenched its emission, while in the aggregate state, the IMR process was impeded, which blocked the non-radiative decay channel and hence made TPE emissive. However, in the conjugated polymer of **P1**, the IMR process of two of the four phenyl rings in the TPE moieties should be limited in some degree, and this peak was therefore still present in the solution state, but very weak. This point, from another side, confirmed that **P1** possessed only AIEE characteristic, not AIE. Thus, it was also explained that this emission of 503 nm was the enhanced TPE-centered emission, however, due to the more conjugative system, the emission was red-shifted than TPE (465 nm). On the other hand, just like normal PF, the conjugated system should give some emission, thus, some blue emissions were observed in the concentrated solutions. Coupled with some intermolecular energy transfer effect, these small peaks in the blue region were completely disappeared in the aggregate state or solid state. The same phenomena were also observed in **P2–P4** (Figs. S12–S16 in supporting information and Table 2): in their solutions, there were two types of very weak fluorescence, while only one peak in their aggregate states accompanying with the enhanced emission. To confirm the presence of the nanoparticles in the mixture solvents, SEM picture of **P1** and **P2** were taken as the examples. As shown in Fig. S17, in the mixture solvent of THF/water (1/9 v/v), both of them formed nano-sized particles.

Table 1
Polymerization results of polymers.

No.	Yield (%)	M_w^a	M_w/M_n^a	T_g^b (°C)	T_d^c (°C)
P1	68.4	10900	1.76	143	363
P2	69.9	5700	1.53	(–) ^d	473
P3	80.3	11000	1.91	(–) ^d	403
P4	59.1	5600	1.66	(–) ^d	420

^a Determined by GPC in THF on the basis of a polystyrene calibration.

^b The glass transition temperature (T_g) of polymers detected by the DSC analyses at a heating rate of 10 °C/min under nitrogen.

^c The 5% weight loss temperature of polymers detected by the TGA analyses at a heating rate of 10 °C/min under nitrogen.

^d Not obtained.

To have a quantitative picture, we estimated the Φ_F values of **P1** using 9,10-diphenylanthracene in cyclohexane ($\Phi_F = 0.9$) as reference. In pure THF, the polymer exhibited negligibly Φ_F value of 9.6×10^{-3} , while at a water content of 99%, the Φ_F value of the polymer dramatically increased to 0.194, 21 fold higher than that in THF solution (Fig. 3 and Table 2). All of the above phenomena showed that the PL behavior of **P1**, using TPE units as important construction block, was changed from ACQ to AIEE active as expected. Similar to **P1**, **P2–P4** were also AIEE active, and the fluorescence quantum yields in aggregate states were enlarged in a large degree in comparison with **P1**.

Fluorescent stability of the polymers was another important parameter with regard to real-world applications. Thus, the annealing experiments of these four polymers were conducted to investigate this property. Taking **P1** as an example: the solid film of **P1** was first baked at 100 °C for 30 min in air, then at 150 °C for another 30 min, followed by 200 °C and so on. Fig. S18 showed the PL emission spectra of **P1** after annealing in air. Because of the aggregation effect or keto formation, the stability of normal PF was poor, and it was reported that thermal treatment of the film of poly(dihexylfluorene) at 100 °C would be unstable in air [12]. However, once TPE was introduced, **P1** was still very stable after

Table 2
Optical properties of polymers in solution and solid state.

No.	$\lambda_{Abs,sol}^a$ (nm)	$\lambda_{PL,sol}^b$ (nm)	$\lambda_{PL,agg}^c$ (nm)	$\lambda_{PL,fil}^d$ (nm)	Φ_{FS}^e	Φ_{FA}^f	Φ_{FA}/Φ_{FS}^g
P1	346	408, 432, 501	503	504	9.6×10^{-3}	0.194	21
P2	366	415, 434, 502	506	510	8.5×10^{-3}	0.334	39
P3	352	408, 434, 507	508	507	8.1×10^{-3}	0.282	35
P4	354	408, 432, 466, 504	506	515	9.8×10^{-3}	0.302	31

^a The absorption wavelength of polymer solutions in pure THF, the concentration was 2×10^{-3} mg/mL.

^b The emission wavelength of polymer solutions in pure THF, the concentration was 2×10^{-3} mg/mL.

^c The emission wavelength of polymer solutions in THF/methanol = 1/9 (V/V), the concentration was 2×10^{-3} mg/mL.

^d The emission wavelength of polymer in films.

^e Quantum yields in THF solutions using 9,10-diphenylanthracene in cyclohexane ($\Phi_F = 90\%$) as standard.

^f Quantum yields in THF/methanol = 1/9 (V/V) using 9,10-diphenylanthracene in cyclohexane ($\Phi_F = 90\%$) as standard.

^g Ratio of fluorescence quantum yields of aggregate and solution.

baked at 150 °C for half an hour, and the PL spectra were almost the same as those tested before annealing. To our surprised, the fluorescent stability of **P2** and **P4** was even better than **P1**, possibly due to their much more rigid structure (Figs. S19–S21).

3.3. Electrochemical characterization

The electrochemical properties of the polymers were investigated by using cyclic voltammetry (CV). The onset oxidation potential of **P1** occur at 0.87 V. Based on the onset potential and according to the equation of $E_{\text{HOMO}} = -(E_{\text{onset(ox),FOC}} + 4.8)$ eV, the HOMO energy level was determined to be -5.67 eV. As the onset reduction potential could not be observed clearly, the LUMO energy level was calculated by the equation of $E_{\text{LUMO}} = (E_{\text{HOMO}} + E_{\text{g}}^{\text{opt}})$ eV, where $E_{\text{g}}^{\text{opt}}$ was the band gap estimated from the absorption spectra of the polymer film. Thus, the LUMO energy level was estimated to be -2.81 eV. The electrochemical data of the other three polymers were also tested and summarized in Table 3. The different copolymer units resulted in different HOMO and LUMO values, further confirming that it was feasible to use different comonomers with different characteristics to adjust the emitting behavior.

3.4. Explosive detection by polymer nanoaggregates

Photoinduced electron transfer (PET) quenching process was usually used to detect nitro aromatic explosives, in particular 2,4,6-trinitrotoluene (TNT) and 2,4,6-trinitrophenol (picric acid, PA), the common toxic and explosive pollutants [13]. For the sake of anti-terrorism and homeland-security implications, sensitive sensors were badly needed. Here, the strong fluorescence of the nanoaggregates of **P1–P4** suspended in the aqueous mixtures made it possible to be utilized as chemosensors toward TNT and PA. Unlike 2,4-dinitrotoluene (DNT) and TNT, PA was commercial availability, thus, it could be used as a model compound to evaluate the sensing property of these polymers.

The explosive probe was prepared as nanoaggregates in the THF/water mixture with 90% water content. After the addition of PA into the aggregate suspension, the fluorescent intensity of **P1** decreased rapidly (Fig. 4A), even at a PA concentration as low as 1.0 $\mu\text{g/mL}$ (1.0 ppm). The fluorescence could be quenched completely at a PA concentration of 50 $\mu\text{g/mL}$ (50 ppm), confirming that the nanoparticle suspension of **P1** could detect nitro aromatic explosives with high sensitivity. The Stern–Volmer plot was nearly linear with a correlation coefficient (R^2) of 0.9855 at the PA concentrations lower than 16 $\mu\text{g/mL}$ (Fig. 4B). Afterward, the curve deviated from linearity and bent upward, suggesting the occurrence of “super-quenching” due to the involvements of self-absorption and/or energy transfer [14]. Also, **P2–P4** could be used as chemosensors similar to **P1**, due to their similar AIEE characteristics. Thanks to their much higher quantum yields than **P1**, the quenching efficiencies of **P2–P4** were much better (Table 4), and **P3** bearing carbazole moieties possessed the best comprehensive performance. In comparison with other TPE-containing

Table 3
Electrochemical properties of polymers.

No.	$E_{\text{g}}^{\text{opt}}$ (eV) ^a	$E_{\text{onset(ox)}}$ (V) vs FOC ^b	E_{HOMO} (eV) ^c	E_{LUMO} (eV) ^d
P1	2.86	0.87	−5.67	−2.81
P2	2.67	0.75	−5.55	−2.38
P3	2.63	0.72	−5.58	−2.95
P4	2.81	0.93	−5.73	−2.92

^a Band gaps obtained from absorption edge ($E_{\text{g}} = 1240/\lambda_{\text{onset}}$).

^b $E_{\text{FOC}} = 0.48$ V vs Ag/AgCl.

^c $E_{\text{HOMO}} = -(E_{\text{onset(ox),FOC}} + 4.8)$ eV.

^d $E_{\text{LUMO}} = (E_{\text{HOMO}} + E_{\text{g}}^{\text{opt}})$ eV.

Table 4
Sensing properties of polymers **P1–P4** in aggregate state.

No.	$C_{\text{discerned}}^{\text{a}}$ (ppm)	$C_{\text{quench}}^{\text{b}}$ (ppm)	Linear range ^c (ppm)	R^2 ^d
P1	1.0	55	<16	0.9855
P2	0.33	52	<16	0.9570
P3	0.17	40	<20	0.9858
P4	0.17	37	<14	0.9662

^a The lowest detectable PA concentration.

^b The lowest PA concentration for the completely quenched fluorescence.

^c The linear detection range of PA concentration.

^d The correlation coefficient of the linear regression equation.

polymers reported in the literature, **P1–P4** demonstrated higher sensitivity, which should be ascribed to the “molecular wire effect” of the conjugated polymers [3,15].

However, for practical applications, using nanoaggregates as probes was not good enough, and it was more convenient to use in the solid state. Thus, test strips were prepared by immersing filter paper into their THF solutions (0.2 mg/mL) and then dried in air, to investigate if these polymers could be direct used in solid state [16]. The obtained papers were dipped into a toluene solution of PA as well as pure toluene. As shown in Fig. 4C, the paper film displayed strong PL upon excitation, however, became nearly nonemissive after dipping into the PA solution. As to **P3** and **P4**, only 50 $\mu\text{g/mL}$ of PA was enough to quench the fluorescence completely. These demonstrated a prototype device using the AIEE polymers for detecting explosives in real-world applications.

3.5. Electroluminescence (EL) properties

As mentioned above, the introduction of the TPE unit to PF main chain was to change the fluorescent behavior of PFs, with aim to avoid the ACQ effect. As well known, PF and its derivatives were promising light-emitting materials. Thus, how about the EL properties of the PLED based on **P1–P4** with AIEE characteristics? To answer this question, we fabricated PLED devices using these polymers as the emitting layers (EML) according to the “standard recipe” for screening tests: ITO/PEDOT:PSS (25 nm)/Poly-TPD (25 nm)/EML (32 nm)/TPBI (35 nm)/Cs₂CO₃ (8 nm):Ag (100 nm). The EL data of PLED devices were summarized in Table 5 and Fig. 5.

The efficiency of **P1**-based PLED was not satisfied with a maximum luminance efficiency of 0.20 cd/A and a maximum brightness of 574 cd/m². If using a twisted structure, spirobifluorene, as comonomer instead of normal fluorene, the efficiency of PLED device has a large improvement: the turn-on voltage was 1.8 V decreased, and the maximum luminescence was up to 1761 cd/m². Furthermore, the luminescence efficiency was more than four times than before. On the other hand, to further improve the EL efficiency, it was critical to achieve both efficient charge injection and balanced mobility of both charge carriers inside the

Table 5
EL data of PLEDs devices.

No.	$\lambda_{\text{EL}}^{\text{a}}$ (nm)	V_{on}^{b} (V)	Lumin ^c L (cd/m ²)	CD ^d J (mA/cm ²)	CE ^e (cd/A)
P1	494	8.7	574 (16.8)	376	0.20
P2	515	6.9	1761 (15.0)	380	0.82
P3	501	5.7	3609 (12.9)	434	1.17
P4	509	4.8	3109 (12.6)	399	1.14

^a The EL spectra of the device.

^b Turn-on voltage.

^c Maximum luminance, while the corresponding operating voltage was given in the parentheses.

^d Current density at the maximum luminescence, also the maximum current density.

^e Maximum luminescence efficiency.

electroluminescent polymers. Carbazole, which was very famous for its good hole-transporting and electroluminescent activities, has been already widely used as important block to construct LED materials [17]. 1,3,4-Oxadiazole derivatives were the famous electron deficient materials with good thermal and chemical stabilities as well as high photoluminescence quantum yields, and generally used as electron-transport materials in PLEDs [18]. Thus, in this paper, we also used these two moieties instead of fluorene unit to construct conjugated polymers **P3** and **P4** to achieve the balance of charge transport, and the results were really better than **P2** as expected. For **P3**-based PLED device, the maximum luminescence was two folds of **P2** with a maximum luminance efficiency of 1.17 cd/A. These results suggested that the incorporation of hole-transporting carbazole units or electron-transporting oxadiazole units was also effective in improving EL performance of the AIEE-based PLED devices, similar to normal PLED devices. However, to know more information about polymers with AIE or AIEE characteristics, more researches were still needed. Also, it should be pointed out that the EL devices of these polymers were not optimized, thus, better performance might be achieved. Anyhow, these preliminary EL results, especially those of **P3** and **P4**, demonstrated the applicability of AIE or AIEE characteristics polymers.

4. Conclusion

In this paper, for the first time, a new series of TPE-containing conjugated polymers **P1–P4** were prepared successfully through simple palladium-catalyzed Suzuki polycondensation reaction, and all polymers exhibited good thermal stabilities ($T_d > 363$ °C) and excellent fluorescent stabilities. As expected, the obtained polymers were AIEE active, thanks to the AIE property of TPE moieties. Their AIEE features made them acting as explosive chemosensors both in the aggregate and solid states with high sensitivity. The PLED devices (ITO/PEDOT:PSS (25 nm)/Poly-TPD (25 nm)/**P1–P4** (32 nm)/TPBI (35 nm)/Cs₂CO₃ (8 nm):Ag (100 nm)) have been fabricated to investigate their electroluminescent properties. Interestingly, owing to the introduced hole-transporting or electron-transporting groups, the EL performance of **P3** and **P4** was improved dramatically, with the maximum luminescence of 3609 cd/m² (**P3**), and the maximum luminescence efficiency as high as 1.17 cd/A (**P3**).

Acknowledgments

We are grateful to the National Fundamental Key Research Program (2011CB932702), and the National Science Foundation of China (no. 21161160556) for financial support.

Appendix A. Supplementary material

Supplementary data related to this article can be found online at doi:10.1016/j.polymer.2012.05.035.

References

- [1] (a) Burroughes JH, Bradley DDC, Brown AR, Marks RN, Mackay K, Friend RH, et al. *Nature* 1990;347:539; (b) Jenekhe SA. *Adv Mater* 1995;7:309; (c) Hide F, Diaz-Garcia MA, Schartz BJ, Heeger AJ. *Acc Chem Res* 1997;30:430; (d) Müller CD, Falcou A, Reckefuss N, Rojahn M, Wiederhorn V, Rudati P, et al. *Nature* 2003;421:829–33; (e) Friend RH, Gymer RW, Holmes AB, Burroughes JH, Marks RN, Taliani C, et al. *Nature* 1999;397:121; (f) Li Z, Ye S, Liu Y, Yu G, Wu W, Qin J, et al. *J Phys Chem B* 2010;114:9101; (g) Wang R, Wang W, Yang G, Liu T, Yu J, Jiang Y. *J Polym Sci Part A* 2008;46:790; (h) Ding L, Bo Z, Chu Q, Li J, Dai L, Pang Y, et al. *Macromol Chem Phys* 2006;207:870;
- (i) Tsai L, Chen Y. *J Polym Sci Part A* 2007;45:4465;
- (j) Peng Q, Yan L, Chen D, Wang F, Wang P, Zou D. *J Polym Sci Part A* 2007;45:5296;
- (k) Liu F, Liu R, Hou X, Xie L, Wu H, et al. *J Polym Sci Part A* 2009;47:6451;
- (l) Wu W, Ye S, Yu G, Liu Y, Qin J, Li Z. *Macromol Rapid Commun* 2012;33:164.
- [2] (a) Pei QB, Yang Y. *J Am Chem Soc* 1996;118:7416–7; (b) Bernius MT, Mike I, O'Brien J, Wu W. *Adv Mater* 2000;12:1737; (c) Scherf U, List EJW. *Adv Mater* 2002;14:477; (d) Kraft A, Grimsdale AC, Holmes AB. *Angew Chem Int Ed* 1998;37:402; (e) Yang RQ, Tian RY, Hou Q, Yang W, Cao Y. *Macromolecules* 2003;36:7453; (f) Leclerc MJ. *Polym Sci Part A* 2001;22:1365.
- [3] (a) Li Z, Lou X, Yu H, Li Z, Qin J. *Macromolecules* 2008;41:7433; (b) Li Z, Lou X, Li Z, Qin J. *ACS Appl Mater Inter* 2009;1:132; (c) Dong S, Ou D, Qin J, Li Z. *J Polym Sci Part A* 2011;49:3314.
- [4] (a) Birks JB. *Photophysics of aromatic molecules*. London: John Wiley & Sons Ltd.; 1970; (b) Jayanty S, Radhakrishnan TP. *Chem Eur J* 2004;10:791; (c) Strehmel B, Sarker AM, Malpert JH, Strehmel V, Seifert H, Neckers DC. *J Am Chem Soc* 1999;121:1226.
- [5] (a) Chiang CL, Tseng SM, Chen C, Hsu C, Shu C. *Adv Funct Mater* 2008;18:248; (b) Yang J, Yan J. *Chem Commun*; 2008:1501; (c) Lim S, Friend RH, Rees ID, Li J, Ma Y, Robinson K, et al. *Adv Funct Mater* 2005;15:981; (d) Fan C, Wang S, Hong JW, Bazan GC, Plaxco KW, Heeger AJ. *Proc Natl Acad Sci USA* 2003;100:6297; (e) Hecht S, Fréchet JM. *Angew Chem Int Ed* 2001;40:74; (f) Moorthy JN, Natarajan P, Venkatakrishnan P, Huang DF, Chow TJ. *Org Lett* 2007;9:5215; (g) Gaylord BS, Wang S, Heeger AJ, Bazan GC. *J Am Chem Soc* 2001;123:6417.
- [6] (a) Hong Y, Häussler M, Lam J, Li Z, Sin K, Dong Y, et al. *Chem Eur J* 2008;14:6428; (b) Liu L, Zhang G, Xiang J, Zhang D, Zhu D. *Org Lett* 2008;10:4581; (c) Luo X, Li J, Li C, Heng L, Dong Y, Liu Z, et al. *Adv Mater* 2011;23:3261; (d) Huang J, Yang X, Wang J, Zhong C, Wang L, Qin J, et al. *J Mater Chem* 2012;22:2478; (e) Wu W, Ye S, Huang L, Xiao L, Fu Y, Huang Q, et al. *J Mater Chem* 2012;22:6374.
- [7] (a) Luo J, Xie Z, Lam JWY, Cheng L, Chen H, Qiu C, et al. *Chem Commun*; 2001:1740; (b) Lee SH, Jang BB, Kafafi ZH. *J Am Chem Soc* 2005;127:9071; (c) Han M, Hara M. *J Am Chem Soc* 2005;127:10951.
- [8] (a) Dong Y, Lam JWY, Qin A, Sun J, Liu J, Li Z, et al. *Chem Commun*; 2007:3255; (b) Li Z, Dong YQ, Lam JWY, Sun J, Qin A, Häussler M, et al. *Adv Funct Mater* 2009;19:905; (c) Zeng Q, Li Z, Dong Y, Di C, Qin A, Hong Y, et al. *Chem Commun*; 2007:70; (d) Dong S, Li Z, Qin J. *J Phys Chem B* 2009;113:434; (e) Li Q, Yu S, Li Z, Qin J. *J Phys Org Chem* 2009;22:241; (f) Li Z, Dong Y, Mi B, Tang Y, Häussler M, Tong H, et al. *J Phys Chem B* 2005;109:10061.
- [9] (a) Shen W, Dodda R, Wu C, Wu F, Liu T, Chen H, et al. *Chem Mater* 2004;16:930; (b) Wong K, Chi L, Huang S, Liao Y, Liu Y, Wang Y. *Org Lett* 2006;8:5029.
- [10] Qin A, Jim C, Tang Y, Lam J, Liu J, Mahtab F, et al. *J Phys Chem B* 2008;112:9281.
- [11] Hong Y, Lam JWY, Tang BZ. *Chem Commun*; 2009:4332.
- [12] Sims M, Bradley DDC, Ariu M, Koeberg M, Asimakis A, Grell M, et al. *Adv Funct Mater* 2004;14:765.
- [13] (a) Fainberg A. *Science* 1992;255:1531; (b) Toal SJ, Trogler WC. *J Mater Chem* 2006;16:2871; (c) Yolanda S, Ramón MM, María DM, Marcos D, Félix S, Ana MC, et al. *Chem Soc Rev* 2012;41:1261.
- [14] Thomas III SW, Joly GD, Swager TM. *Chem Rev* 2007;107:1339.
- [15] (a) Lam JWY, Tang BZ. *Acc Chem Res* 2005;38:745; (b) Wu W, Ye S, Yu G, Liu Y, Qin J, Li Z. *Macromol Rapid Commun* 2012;33:164; (c) Whitcombe MJ, Chianella I, Larcombe L, Piletsky SA, Noble J, Porter R, et al. *Chem Soc Rev* 2011;40:1547; (d) Feng X, Liu L, Wang S, Zhu D. *Chem Soc Rev* 2010;39:2411; (e) Ahn DJ, Kim JM. *Acc Chem Res* 2008;41:805; (f) Haupt K, Mosbach K. *Chem Rev* 2000;100:2495; (g) Swager TM. *Acc Chem Res* 1998;31:201; (h) Liu B, Yu WL, Pei J, Liu SY, Lai YH, Huang W. *Macromolecules* 2001;34:7932.
- [16] Sanchez JC, Trogler WC. *J Mater Chem* 2008;18:3143.
- [17] (a) Shen JY, Yang XL, Huang TH, Lin JT, Ke TH, Chen LY, et al. *Adv Funct Mater* 2007;17:983; (b) Thomas KRJ, Velusamy M, Lin JT, Tao YT, Chuen CH. *Adv Funct Mater* 2004;13:387; (c) Li J, Liu D, Li Y, Lee CS, Kwong HL, Lee ST. *Chem Mater* 2005;17:1208; (d) Zhao Z, Xu X, Wang H, Lu P, Gui Yu, Liu Y. *J Org Chem* 2008;73:594; (e) Thomas KRJ, Lin JT, Tao YT, Ko CW. *J Am Chem Soc* 2001;123:9404.
- [18] (a) Chen SH, Chen Y. *Macromolecules* 2005;38:53; (b) Yu WL, Meng H, Pei J, Huang W, Li Y, Heeger AJ. *Macromolecules* 1998;31:4838; (c) Zhan X, Liu Y, Wu X, Wang S, Zhu D. *Macromolecules* 2002;35:2529; (d) Mikroyannidis JA, Gibbons KM, Kulkarni AP, Jenekhe SA. *Macromolecules* 2008;41:663.